

Influence of Precipitation Sequence on the 3D TaC + Ta₂C/Ta₄C₃ Microstructure Processed by Vacuum Plasma Spraying

R.A. Morris*, D. Butts**, P.A. Shade***, and G.B. Thompson*

* Department of Metallurgical and Materials Engineering, University of Alabama
301 7th Avenue, 116 Houser Hall, Tuscaloosa, AL 35487-0202

** Plasma Processes Inc. 4919 Moores Mill Road, Huntsville, AL 35811

***Universal Technology Corp. 1270 North Fairfield Rd, Dayton, OH 45432

The γ -TaC phase has a melting temperature near 4000°C and is one of the highest melting temperatures known [1]. The precipitation of substoichiometric Ta-rich phases, such as α/β -Ta₂C and ξ -Ta₄C₃, with similar high melting points, provides ample opportunities to tailor the microstructure for improved thermo-mechanical behavior. Vacuum plasma spraying (VPS) was used to fabricate a multi-phase structure of tantalum carbides as a function of chemistry and solidification route. During the VPS process, TaC powder was melted under a plasma arc and rapidly solidified onto a graphite mandrel. The loss of carbon was controlled by the resonance time the powder spent in the plasma. These samples were then hot isostatically pressed to homogenize the composition and densify the material. The solidification route with the subsequent precipitation of different Ta-rich substoichiometric phases can be used to modify the microstructure in the thermodynamic two-phase regime, figure 1. This work has explored how the precipitation of the multiple phases developed and controlled the resulting microstructure.

Post processing, the specimens were characterized by X-ray and electron diffraction for phase identification. The specimens were then mounted and a 10 μm x 10 μm x 10 μm isolated pillar was cut out of the edge of the specimen for serial sectioning. A protective platinum cap, ~ 5 μm , was deposited onto the surface of the pillar. This pillar was then focus ion beam (FIB) milled at 1 nA in a FEI Quanta 3D dual beam FIB at steps sizes of 100 nm. The milled surface was then imaged after each consecutive cut using ion contrast imaging. The collected images were then compiled to generate a 3D rendering of the phase and grain morphology.

A comparison of figures 2 and 3 clearly revealed two distinct microstructures. The former consists of an acicular grain morphology with the laths running parallel to the long-axis of the grains where as the latter formed equiaxed grains with secondary phase laths encased at a variety of directions within the grains. The laths have been identified to be either Ta₂C or Ta₄C₃. These phases have the following orientation relationship (OR): $\{111\}_{\text{TaC}} // \{0002\}_{\text{Ta}_4\text{C}_3} // \{0002\}_{\text{Ta}_2\text{C}}$ and $\langle 110 \rangle_{\text{TaC}} // \langle 11\bar{2}0 \rangle_{\text{Ta}_4\text{C}_3} // \langle 11\bar{2}0 \rangle_{\text{Ta}_2\text{C}}$ [2]. The closed packed planes and closed packed directions provided a low misfit interface between the phases; consequently, a low energy growth surface. For the Ta-rich side of the two phase regime (#1 in figure 1), 3D reconstruction revealed that these laths spanned the entire interior of the grain, figure 2(b). In contrast, the C-rich side of the two phase regime (#2 in figure 1), revealed that the laths, which were tens of nanometers in thickness, partially and fully spanned the interior of the grain, figure 3(b). This difference likely resulted from the sequence of precipitation of the secondary phase. If the liquid phase is supercooled for path #1 in figure 1, the liquid would decompose into the two solid phases of TaC and Ta₂C. This liquid decomposition would yield a eutectic-like precipitated microstructure, *i.e.* a layered sequence of the two solid phases.

The low energy interface given by the OR relationship would also provide an anisotropic growth rate in different directions and facilitate the acicular grain morphology. The 3D reconstructions also indicated that these acicular grains have multiple nodes that form from the sides of the primary grain, figure 2(b). For the solidification route #2 in figure 1, the single phase TaC initially formed and then a solid state phase transformation of the sub-stoichiometric phases resulted within the grains. This would explain the variety of multiple orientations of the laths within the grains, *i.e.* precipitation off of different $\{111\}$ TaC planes. A 130° STEM-HAADF tilt series with 2° step sizes for this specimen was collected on a FEI F20 Tecnai (S)TEM. These images were compiled into a 3D reconstruction, figure 3(c). Unlike the FIB-based serial sectioning, which may not resolve all the laths, the complimentary STEM-HAADF collection allowed the fine scale laths to be easily viewed in 3D. Since the secondary phases formed subsequent to the solidification of the primary TaC grains, their influence on morphology of the TaC grain shape was limited. Using 3D characterization, the morphology from the sequence of secondary phase precipitation in the tantalum carbide microstructure was elucidated.

References:

- [1] E K Storms, "The Tantalum-Tantalum Carbide System," in *The Refractory Carbides*: Academic Press, 1967.
 [2] D. J. Rowcliffe and G. Thomas, "Structure of Non-Stoichiometric TaC," *Materials Science and Engineering*, 18(1975) 231-238.
 [3] The work was supported by ARO-W911NF-08-1-0300

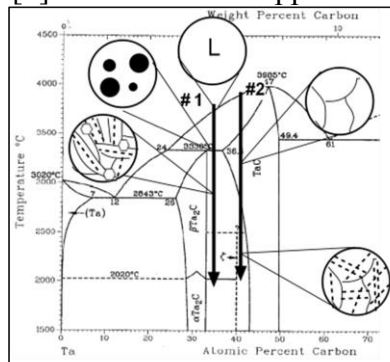


Fig. 1: Binary phase diagram showing compositions used and the solidification routes predicted.

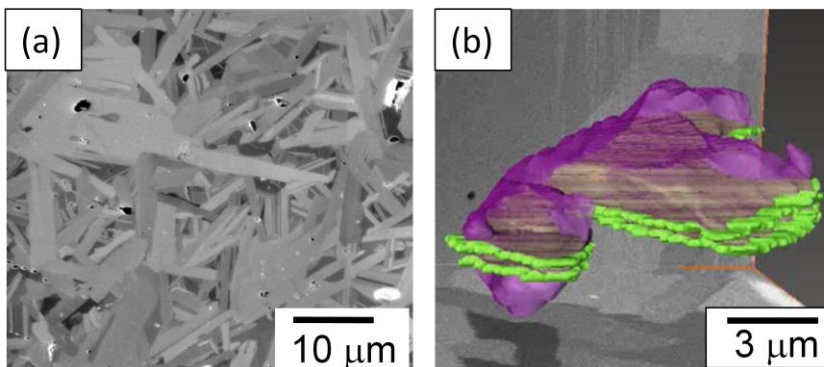


Fig. 2 (a) Ion contrast image from #1 route/fig. 1 **(b)** 3D reconstruction of laths (green) throughout a single grain (purple)

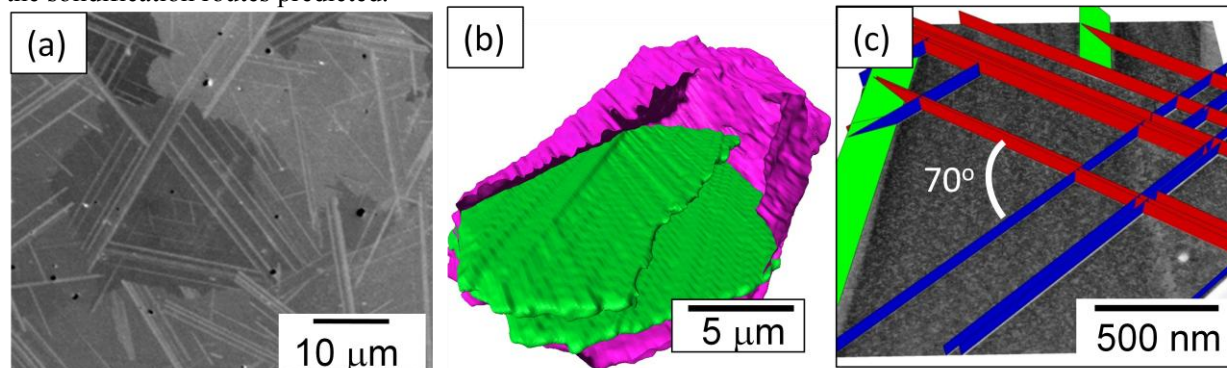


Fig. 3: (a) Ion contrast image from #2 route/fig. 1 (b) 3D reconstruction of laths (green) in a single grain (purple), note that the upper lath terminates in the grain (c) STEM-HAADF tomography tilt series with reconstruction. The different color laths indicated different orientations of the secondary phases in the TaC grain. The angle between laths is 70° , consistent with the different $\{111\}$ orientations.